

## Analysis of the temperature dependence of the forward voltage characteristics of GaInN light-emitting diodes

David S. Meyaard,<sup>1</sup> Jaehee Cho,<sup>1,2,a)</sup> E. Fred Schubert,<sup>1</sup> Sang-Heon Han,<sup>3</sup> Min-Ho Kim,<sup>3</sup> and Cheolsoo Sone<sup>3</sup>

<sup>1</sup>*Future Chips Constellation, Department of Electrical, Computer, and Systems Engineering, Rensselaer Polytechnic Institute, Troy, New York 12180, USA*

<sup>2</sup>*School of Semiconductor and Chemical Engineering, Semiconductor Physics Research Center, Chonbuk National University, Jeonju 561-756, Korea*

<sup>3</sup>*LED Business, Samsung Electronics, Yongin 446-920, Korea*

(Received 18 March 2013; accepted 3 September 2013; published online 18 September 2013)

The forward voltage characteristics of GaInN light-emitting diodes are studied in the temperature range of 80 K to 450 K. The forward-voltage-vs.-temperature curve has a “two-slope” characteristic with a slope of  $dV_f/dT = -1.7$  mV/K and  $-8.0$  mV/K at room temperature and cryogenic temperatures, respectively. To investigate the two-slope characteristic, we perform transmission-line-model measurements on p-type GaN and show that both p-type contact and sheet resistance decrease drastically with increasing temperature. We conclude that  $dV_f/dT$  in the high-slope region is limited by p-type sheet and contact resistance, and in the low-slope region by the GaN pn junction properties. © 2013 AIP Publishing LLC. [<http://dx.doi.org/10.1063/1.4821538>]

GaN-based light-emitting diodes (LEDs) are becoming common in lighting applications, both commercial and residential. Many of these applications, such as automotive lighting or street lighting, are outdoors and subject to great temperature variations. In such applications, it is advantageous for LEDs to have stable performance characterized by a weak temperature dependence of light-output as well as forward voltage. Currently, LEDs suffer from decreasing light-output-power as the temperature increases. This is due to both increased Shockley-Read-Hall recombination, as well as increased electron leakage out of the active region.<sup>1</sup> Such characteristics are undesired, but can be mitigated by reducing the concentration of non-radiative recombination centers in the active region of the LED,<sup>2</sup> or by an LED structure that is designed to limit electron overflow out of the active region.<sup>3</sup> Furthermore, in many applications, LEDs are operated at high current densities, leading to self-heating. If an LED heats up, its forward-voltage-vs.-current characteristic changes, thereby requiring adjustment of the LED’s electrical operating point. Xi *et al.* derived an expression for  $dV_f/dT$  for pn junctions and obtained a room-temperature value for  $dV_f/dT$  of  $-1.8$  mV/K and  $-1.2$  mV/K for lightly doped GaN pn junctions and moderately doped GaAs pn junctions, respectively.<sup>4</sup> Furthermore, the authors acquired data on the forward voltage of GaN UV LEDs and used the data to measure the junction temperature under various bias conditions.<sup>4</sup>

In the present report, we measure the temperature dependence of forward voltage in a GaInN blue LED emitting at 440 nm over a wide range of temperatures (80 K–450 K). We find that the forward-voltage-vs.-temperature curve has a “two-slope” characteristic with a lower slope occurring at room temperature but a significantly higher slope occurring at cryogenic temperatures. We find that the contact and sheet resistances of p-type GaN increase exponentially as the temperature decreases and that this increase plays a significant

role in the forward voltage required to operate the LED at cryogenic temperatures.

The LEDs used in our experiments are grown by metal-organic chemical vapor deposition (MOCVD) and have five GaInN/GaN quantum wells which emit at a peak wavelength of 440 nm. The LED structure employs a p-type AlGaIn electron-blocking layer (EBL) having an Al mole fraction of 15%. Thin-film LEDs are fabricated by bonding the epitaxial side of the LED wafer to a Si wafer and utilizing laser-lift-off to remove the sapphire substrate. The exposed N-face GaN is then surface roughened to enhance light extraction. The thin-film LED wafer is diced into  $1 \times 1$  mm<sup>2</sup> chips that are left unpackaged. A chip is mounted with thermal grease inside a liquid-nitrogen-cooled cryostat to ensure a good thermal contact.

Figure 1(a) shows typical I–V characteristics of an LED as a function of temperature. As the temperature is increased, the forward voltage decreases. The figure elucidates that at cryogenic temperatures (80 K), the change in forward voltage, i.e.,  $dV_f/dT$ , is much greater than at high temperatures. Fig. 1(b), which shows the forward voltage of the LED at 20 mA and 100 mA, reveals two distinct slopes: at room temperature and above, the slope is approximately  $-1.7$  mV/K, whereas at temperatures less than 200 K, the slope is approximately  $-8.0$  mV/K.

First, we present a theoretical expression for the temperature dependence of forward voltage in an LED. The change in forward voltage over a pn junction is given by<sup>4</sup>

$$\frac{dV_j}{dT} = \left( \frac{qV_j - E_g}{qT} + \frac{1}{q} \frac{dE_g}{dT} - \frac{3k}{q} \right), \quad (1)$$

where  $V_j$  is the junction voltage,  $E_g$  is the bandgap energy,  $q$  is the elementary charge, and  $k$  is Boltzmann’s constant. The first summand,  $(qV_j - E_g)/qT$ , is due to the temperature dependence of the intrinsic carrier concentration. The second summand,  $(1/q)(dE_g/dT)$ , describes the temperature dependence of bandgap energy. The third summand,  $-3k/q$ ,

<sup>a)</sup>E-mail: cho.jaehee@gmail.com

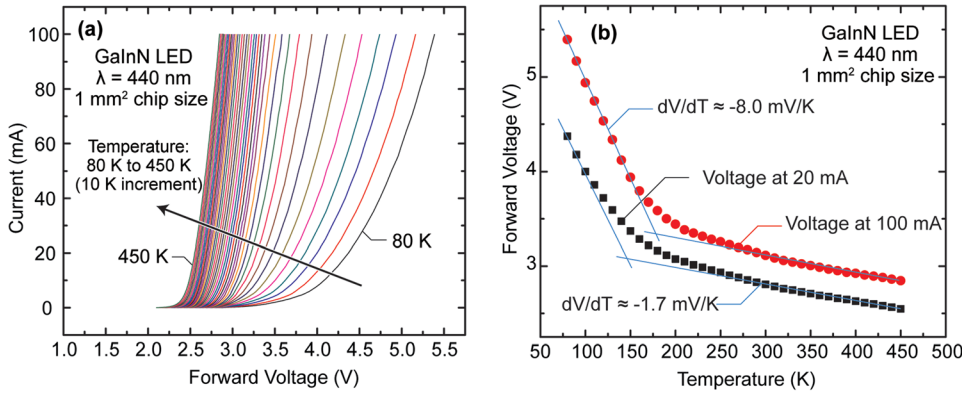


FIG. 1. (a) Current-voltage characteristics of 440 nm GaInN LED measured from 80 to 450 K with 10 K increments. (b) Forward voltage as a function of temperature for an injection current of 20 and 100 mA.

is due to the temperature dependence of  $N_c$  and  $N_v$ , which are the effective density of states in the conduction band and valence band, respectively. Using the appropriate physical constants and GaN material constants for the above equation, the change in junction voltage can be expressed as<sup>4,5</sup>

$$\frac{dV_j}{dT} \approx \frac{k}{q} \ln \left( \frac{N_D N_A}{N_c N_v} \right) - \frac{\alpha T (T + 2\beta)}{q(T + \beta)^2} - \frac{3k}{q}, \quad (2)$$

where  $N_D$  and  $N_A$  are the concentration of donors and acceptors, respectively, and  $\alpha$  and  $\beta$  are the Varshni parameters. For GaN,  $\alpha = 0.566 \text{ meV/K}^2$  and  $\beta = 738 \text{ K}$ .<sup>6</sup> Considering the density of states at 300 K, and assuming doping concentrations of  $N_A = 1 \times 10^{18} \text{ cm}^{-3}$  and  $N_D = 5 \times 10^{18} \text{ cm}^{-3}$ , the value of  $dV_j/dT$  for GaN pn junctions is calculated to be  $-1.2 \text{ mV/K}$ , similar to the measured value around room temperature, as shown in Fig. 1(b). This value serves as a lower bound for the change in forward voltage, since it neglects the LED's series resistance and its dependence on temperature. We include the temperature dependence of the LED's series resistance as the second parenthesized term in the following equation:<sup>5</sup>

$$\frac{dV_f}{dT} = \left( \frac{qV_j - E_g}{qT} + \frac{1}{q} \frac{dE_g}{dT} - \frac{3k}{q} \right) - \frac{1}{2} I \left( \frac{E_a + 2S_p kT}{kT^2} R_{sp} + \frac{E_d + 2S_n kT}{kT^2} R_{sn} \right), \quad (3)$$

where  $E_a$  and  $E_d$  are the activation energy of the Mg acceptor (about 170 meV) and Si donor (about 20 meV), respectively, and  $R_{sp}$  and  $R_{sn}$  are the series resistances of the p- and n-type quasi-neutral regions and contacts, respectively. The parameters  $S_n$  and  $S_p$ , in the high-temperature range, where phonon scattering dominates, are negative quantities, close to  $-3/2$ , representing the temperature dependence of the free-carrier mobility (i.e.,  $\mu \propto T^S$ ). At low temperature, where impurity scattering dominates,  $S_n$  and  $S_p$  are positive values and range between about  $1/2$  and  $2$ . At room temperature,  $R_{sp}$  and  $R_{sn}$  may be of the same order of magnitude. However, because the ionization energy for donors is much smaller than acceptors, the p-type GaN will make a greater contribution to  $dV_f/dT$ . We can therefore neglect the contribution from the series resistance from the n-type term, simplifying Eq. (3) to

$$\frac{dV_f}{dT} = \left( \frac{qV_j - E_g}{qT} + \frac{1}{q} \frac{dE_g}{dT} - \frac{3k}{q} \right) - \left( \frac{1}{2} \frac{E_a + 2S_p kT}{kT^2} I R_{sp} \right). \quad (4)$$

According to Eq. (4), a lower series resistance will reduce the slope  $dV_f/dT$ . Two drastically different slopes are displayed in Fig. 1(b): at cryogenic temperature (80–150 K),  $dV_f/dT \approx 8.0 \text{ mV/K}$ ; above room temperature,  $dV_f/dT \approx 1.7 \text{ mV/K}$ . These two very different slopes indeed suggest the presence of two distinctly different physical mechanisms. Due to the presence of the two distinct slopes and because the ionization energy of Mg acceptors is around 170 meV (so that very few acceptors are ionized at low temperatures), we hypothesize that the p-type series resistance and the pn junction is the determining factor for the  $dV_f/dT$  slope at cryogenic and room temperature, respectively.

In order to confirm our hypothesis regarding the effect of the p-type series resistance on  $dV_f/dT$ , the resistivity of the p-type GaN is assessed by means of temperature dependent transmission line model (TLM) measurements<sup>7</sup> that are performed over a wide range of temperatures. The sample, a 200 nm p-type GaN layer with Mg concentration of  $5 \times 10^{19} \text{ cm}^{-3}$ , is epitaxially grown by MOCVD. The p-type GaN is patterned using standard photolithography, using both circular<sup>8</sup> and linear TLM patterns with various contact separations. To form an ohmic p-type contact, a metal stack of NiZn/Ag (5/200 nm) is deposited on the p-type GaN by electron-beam evaporation. This metal stack has a small Schottky-Mott barrier height, consistent with the design rules presented by Mohammad.<sup>9</sup> The measured I-V curves show near-ideal ohmic behavior at all measurement temperatures. An Agilent 4155C parameter analyzer is used to measure the I-V characteristics of the TLM patterns. Figure 2 shows the measured total resistance as a function of TLM gap size and temperature. Although for large gaps in the linear TLM pattern (without a mesa etch), current spreading can occur, the measured linear and circular (after the correction factor is applied<sup>8</sup>) TLM patterns yield similar results. Three curves are plotted on a semi-logarithmic scale in order to accommodate the large (several orders of magnitude) differences in the p-type layer and contact resistances.

For high-quality ohmic contacts, the value of the contact resistance,  $R_c$ , is much smaller than the resistance of the semiconductor. Using a linear fit to the experimental data shown in Fig. 2, the contact resistance,  $R_c$ , and the p-type layer sheet resistance,  $R_s$ , are determined. The values of  $R_c$  and  $R_s$  are

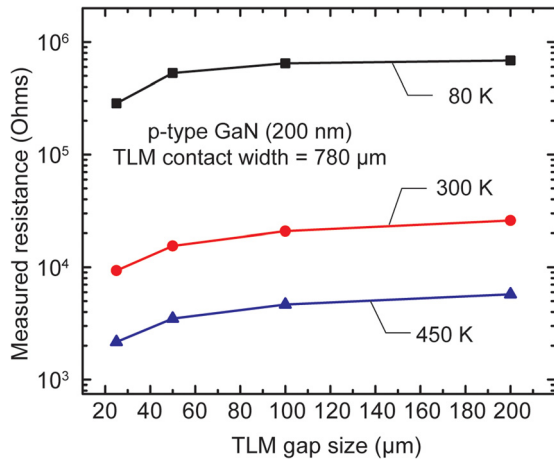


FIG. 2. Resistance of p-type GaN as a function of TLM gap size measured at 80, 300, and 450 K. The total resistance varies by orders of magnitude within this temperature range.

shown in Fig. 3, displaying an exponentially increasing trend with decreasing temperature. The figure elucidates that both  $R_C$  and  $R_S$  have a very strong temperature dependence, with very high resistance values at low temperatures. Decreasing contact resistance with increasing temperature is consistent with previous reports of ohmic contacts to GaN.<sup>10,11</sup>

We next present theoretical explanation for the shape of these curves, beginning with the p-type contact resistance. In general, the current in a metal-semiconductor contact may be transported by five different mechanisms:<sup>12</sup> (1) thermionic emission of carriers over the Schottky barrier, (2) tunneling of carriers through the barrier, (3) recombination of carriers in the space-charge region, (4) diffusion of carriers into the depletion region, and (5) carriers injected from the metal that diffuse into the semiconductor. Of these, the most significant are (1) thermionic emission and (2) tunneling. If there is no change in resistance as a function of temperature, tunneling is likely the dominant mechanism for transport; if a large change is seen, thermionic emission is likely the main transport mechanism for the p-metal contact. At the lowest temperatures measured (80 and 100 K), the change in contact resistance is relatively small. Due to a lack of temperature dependence, the transport through the contacts is likely

dominated by a tunneling mechanism. Because we observe a strong temperature dependence of  $R_C$  at temperatures above 200 K, we assume that thermionic emission is dominant in this region. The thermionic portion of the current can be described by the following equation:<sup>12</sup>

$$J = A^{**}T^2 \exp\left(-\frac{q\phi_B}{kT}\right) \left[ \exp\left(\frac{qV}{kT}\right) - 1 \right], \quad (5)$$

where  $A^{**}$  is the effective Richardson constant,  $\phi_B$  is the energy of the Schottky barrier height,  $q$  is the elementary charge, and  $V$  is the voltage applied to the contact. For an ohmic contact, this translates to a contact resistance of

$$R_C = \frac{k}{A^{**}Tq} \exp\left(\frac{q\phi_B}{kT}\right). \quad (6)$$

From this equation,  $R_C$  has an exponential dependence on temperature. This is consistent with the experimental results obtained from the TLM study shown in Fig. 3(a).

At room temperature, because the ionization energy of acceptors in GaN is very high, about 170 meV for Mg acceptors, the p-type GaN is in the ionization regime (also called freeze-out regime). In this regime, the hole concentration is given by<sup>13</sup>

$$p \approx \left(\frac{1}{g_a} N_A N_V\right)^{\frac{1}{2}} \exp\left(-\frac{E_a}{2kT}\right), \quad (7)$$

where  $g_a$  is the ground state degeneracy for acceptors, 4 in GaN. The resistivity of a p-type semiconductor is given by  $\rho = 1/q\mu_p p$ , so the sheet resistance depends exponentially on temperature:

$$R_S \propto \exp\left(\frac{E_a}{2kT}\right) \quad (8)$$

Figure 3(b) shows the sheet resistance of p-type GaN, as extracted from the TLM measurement. The figure is made on a semi-logarithmic plot so that the exponential trend can be easily observed.

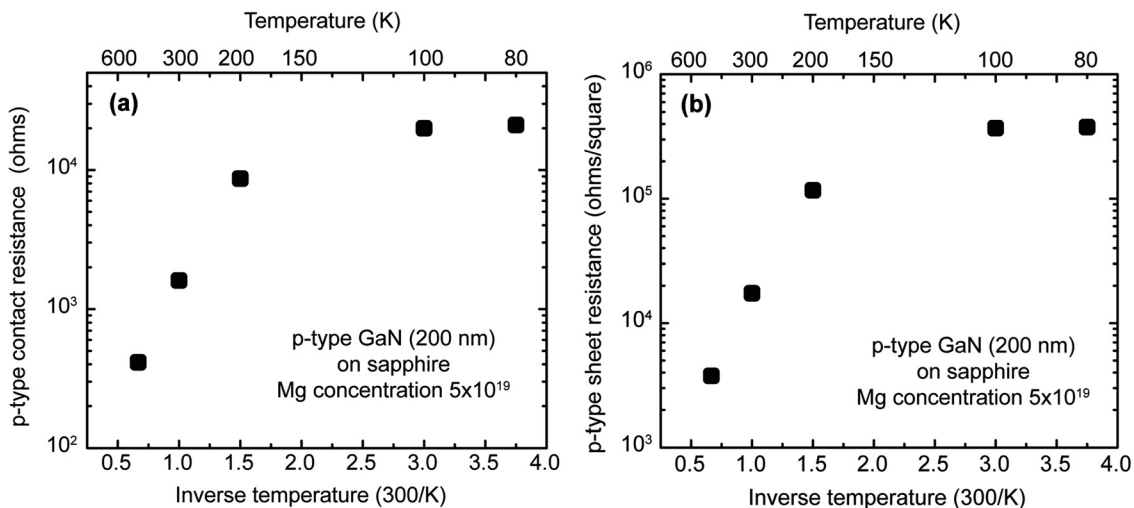


FIG. 3. (a) Contact resistance and (b) sheet resistance of p-type GaN as a function of temperature, as extracted from TLM measurements.

Figures 3(a) and 3(b) show that both the contact and sheet resistance have a distinct transition in slope around 200 K, replicating a similar trend as the LED forward voltage. Previously, it has been shown that the formation of good ohmic contacts to GaN is heavily dependent on the free carrier concentration immediately below the metal contact, as well as the metal-semiconductor barrier height.<sup>14</sup> Therefore, the reason for the slope transition at 200 K is likely the freeze-out of holes, which significantly increases both the contact and sheet resistance. It is clear that, at temperatures lower than 200 K, the series resistance contribution to the forward voltage in Eq. (4) is dominant, resulting in a strong temperature dependence of the forward voltage (high slope of  $dV_f/dT$ ).

In conclusion, experiments on the temperature dependence of the forward voltage in GaInN blue LEDs reveal a pronounced “two-slope” characteristic. The two-slope characteristic is explained by two physical mechanisms: The room-temperature slope ( $-1.7$  mV/K) is determined by physical properties of the GaN pn junction, including the density of states, the bandgap energy, as well as the p- and n-type doping concentrations. The cryogenic-temperature slope ( $-8$  mV/K) is determined by p-type layer characteristics including the p-type series and contact resistance. When the contact resistance of p-type GaN are measured as a function of temperature,  $R_c$  exhibits a relatively small dependence on temperature (80 and 100 K), indicating that tunneling is the dominant mechanism for carrier transport. As the temperature is increased (above 200 K), thermionic emission over the barrier becomes important resulting in an exponential decrease of  $R_c$  with increasing temperature. These two dependences support the assignment of the two-slope characteristic.

The authors gratefully acknowledge support by Samsung Electronics Company, Sandia National Laboratories (SNL), Department of Energy, and Applied Materials – Varian Semiconductor Equipment. J. Cho acknowledges support by the Basic Research Laboratory Program (2011-0027956) and Priority Research Centers Program (2009-0094031) through the National Research Foundation of Korea funded by the Ministry of Education, Science and Technology. The authors also gratefully acknowledge Sauvik Chowdhury for p-type GaN sample preparation.

- <sup>1</sup>D. S. Meyaard, Q. Shan, Q. Dai, J. Cho, E. F. Schubert, M.-H. Kim, and C. Sone, *Appl. Phys. Lett.* **99**, 041112 (2011).
- <sup>2</sup>S. Chhajed, J. Cho, E. F. Schubert, J. K. Kim, D. D. Koleske, and M. H. Crawford, *Phys. Status Solidi A* **208**, 947 (2011).
- <sup>3</sup>M. F. Schubert, J. Xu, J. K. Kim, E. F. Schubert, M. H. Kim, S. Yoon, S. M. Lee, C. Sone, T. Sakong, and Y. Park, *Appl. Phys. Lett.* **93**, 041102 (2008).
- <sup>4</sup>Y. Xi and E. F. Schubert, *Appl. Phys. Lett.* **85**, 2163 (2004).
- <sup>5</sup>Y. Xi, T. Gessmann, J. Xi, J. K. Kim, J. M. Shah, E. F. Schubert, A. J. Fischer, M. H. Crawford, K. H. A. Bogart, and A. A. Allerman, *Jpn J. Appl. Phys.* **44**, 7260 (2005).
- <sup>6</sup>M. O. Manasreh, *Phys. Rev. B* **53**, 16425 (1996).
- <sup>7</sup>G. K. Reeves and H. B. Harrison, *IEEE Electron Device Lett.* **3**, 111 (1982).
- <sup>8</sup>G. S. Marlow and M. B. Das, *Solid State Electron.* **25**, 91 (1982).
- <sup>9</sup>S. N. Mohammad, *J. Appl. Phys.* **97**, 063703 (2005).
- <sup>10</sup>Z. H. Liu, S. Arulkumaran, and G. I. Ng, *Appl. Phys. Lett.* **94**, 142105 (2009).
- <sup>11</sup>F. Lin, B. Shen, S. Huang, F. J. Xu, L. Lu, J. Song, F. H. Mei, N. Ma, Z. X. Qin, and G. Y. Zhang, *J. Appl. Phys.* **105**, 093702 (2009).
- <sup>12</sup>S. M. Sze and K. K. Ng, *Physics of Semiconductor Devices*, 3rd ed. (Wiley & Sons, Inc., Hoboken, 2007), 153 pp.
- <sup>13</sup>H. Morkoç, *Nitride Semiconductors and Devices* (Springer-Verlag, Berlin, 1999).
- <sup>14</sup>F. Iucolano, F. Roccaforte, A. Alberti, C. Bongiorno, S. Di Franco, and V. Raineri, *J. Appl. Phys.* **100**, 123706 (2006).